Imaging electron molecular orbitals via ionization by intense femtosecond pulses

G. Lagmago Kamta and A. D. Bandrauk
Département de Chimie, Université de Sherbrooke, Sherbrooke, Québec, Canada J1K 2R1
(Received 2 June 2006; published 28 September 2006)

We report an *ab initio* investigation of the ionization of an oriented molecule (H_2^+) by intense linearly polarized laser pulses, using initial states (i.e., the active orbitals) having various symmetries and electron distributions. We show that the orientation dependence of the total (nondifferential) ionization probability of a molecule is very sensitive to the electron distribution within the active orbital. This sensitivity is strong enough that by collecting the ionization probability for various molecular orientations relative to the laser polarization, one can infer the electron distribution within the active orbital. The ionization of oriented molecules by intense low frequency fields can be a tool for imaging electron densities in active molecular orbitals.

DOI: 10.1103/PhysRevA.74.033415 PACS number(s): 33.80.Rv, 33.80.Wz, 33.80.Eh, 42.50.Hz

I. INTRODUCTION

Many techniques that aim at extracting details on molecular wave functions have been proposed in the literature. Kinetic energy spectra of protons originating from Coulomb explosion of the H_2^+ molecules have been used to reconstruct the initial nuclear probability distribution [1]. To some extend, Scanning tunnelling microscope [2] and electron momentum spectroscopy [3] can be used to obtain the density of electrons in molecular orbitals. A recently proposed tomographic imaging technique [4] permits to obtain the full three-dimensional (3D) shape of a molecular orbital. A key ingredient of this technique is the high-order harmonic emission by the molecule via the recollision mechanism [5].

Studies of the ionization of molecules indicate that it can be very different from that of atoms, thanks to additional symmetries and complexity in molecules. For example, enhanced ionization occurs in molecules as they stretch to larger internuclear distances [6–8], and molecular ionization depends strongly on the orientation of the molecule relative to the polarization of the laser [8–12]. Also, depending on the symmetry of the active orbital or the highest occupied molecular orbital (HOMO), interferences of contributions from various nuclei can lead to a suppression of ionization in certain molecules, compared to atoms with similar ionization potentials [13–15].

The study of the orientation dependence of molecular ionization has attracted significant attention lately [8–12], thanks to improvements in molecular orientation and alignment techniques [16], which has lead to experiments with aligned and oriented molecules. Pump-probe techniques are commonly used, where a first low intensity laser pulse (the pump) aligns the molecule, and a second laser pulse (the probe) of higher intensity ionizes the molecule. An important issue here is not only to understand the influence of molecular orientation on molecular ionization, but also the influence of various symmetries and electron distributions within the active molecular orbital.

Most theoretical studies of the orientation dependence of molecular ionization are based on approximate approaches such as the KFR (see Ref. [15] and references therein) and the molecular ADK [12] models. These approaches neglect the influence of the Coulomb potential, as well as the potential role of intermediate excited states. Recently, we have developed an *ab initio*, nonperturbative approach to solving the 3D time-dependent Schrödinger equation (TDSE) for diatomic molecules interacting with intense laser fields having an arbitrarily orientated polarization [10,11,17]. The only approximations made in this approach are the fixed nuclei and the dipole approximation. In this paper, we use this *ab initio* approach to investigate the sensitivity of the orientation dependence of molecular ionization to the symmetry and the electron distribution in active molecular orbitals. We consider various laser frequencies, intensities and pulse durations, and use initial states (active orbitals) having various symmetries and angular momenta. We find that the total (nondifferential) ionization probability vs the orientation angle θ depends strongly on the symmetry and the electron distribution within the active orbital. In addition, results indicate that from the total ionization probability obtained for various orientation angles θ, one can reconstruct the contour of the spatial electron distribution in the active orbital.

This paper is organized as follows. In Sec. II we show, using four low lying states of H_2^+ (i.e., $1s\sigma_g$, $1s\sigma_u$, $2p\pi_u$, and $2p\pi_g$) as active orbitals, that the orientation dependence of the ionization probability mimics the contour of the electron distribution in the active orbital. This is confirmed by our investigation of the role of the internuclear distance in Sec. III. A short conclusion is given in Sec. IV.

II. IMAGING ELECTRON DENSITIES IN MOLECULAR ORBITAL

The TDSE for H_2^+ in a laser field is

$$i\frac{\partial}{\partial t}\Psi(\mathbf{r},t) = [H + \mathbf{A}(t)\cdot\mathbf{p}]\Psi(\mathbf{r},t), \tag{1}$$

where $\mathbf{p}$ denotes the electron momentum,

$$H = \frac{\mathbf{p}^2}{2} - \frac{1}{|\mathbf{r}+\mathbf{R}/2|} - \frac{1}{|\mathbf{r}-\mathbf{R}/2|} \tag{2}$$

is the electronic Hamiltonian, and R is the internuclear distance. Atomic units (a.u.) are used.

We make the following choices that are convenient but do not impose any restriction on the system: (i) the z axis is along the internuclear axis of the molecule; (ii) the (y,z) plane contains the linear polarization of the laser, whose potential vector can be written as $\mathbf{A}(t)=A_0 f(t)\sin(\omega t)\mathbf{e}$, where

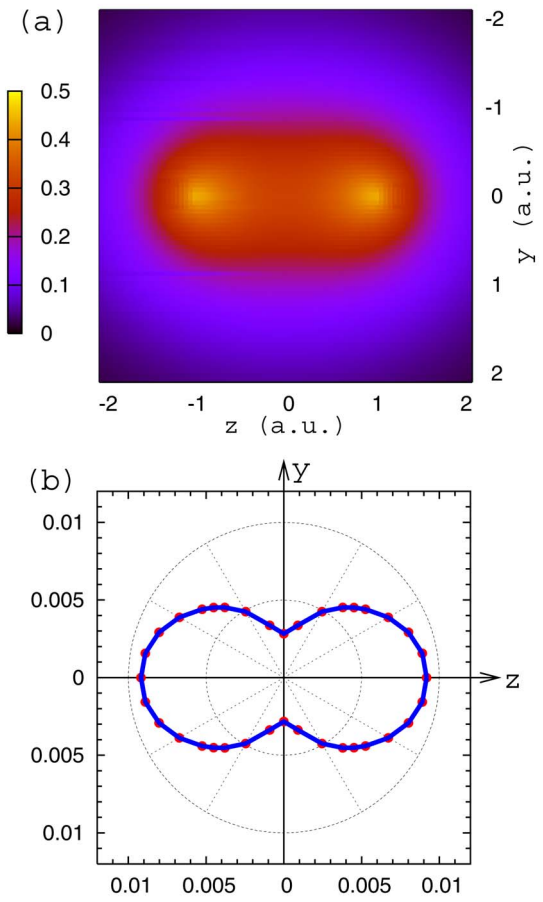

FIG. 1. (Color online) (a) Contour plot, in the (y,z)-plane, of the electronic wave function $\Psi(y,z)$ for the $1s\sigma_g$ state of H_2^+. The nuclei are located along the z axis at $z=-1$ and $z=+1$. (b) Polar coordinate representation of the ionization probability of H_2^+ (initially in the $1s\sigma_g$ state) vs the orientation angle θ. Laser parameters are $I=5\times10^{14}$ W/cm^2, $\omega=0.057$ a.u., and the total pulse duration is 26 fs. Here and in subsequent figures, dots represent the calculated data and lines are drawn to guide the eye.

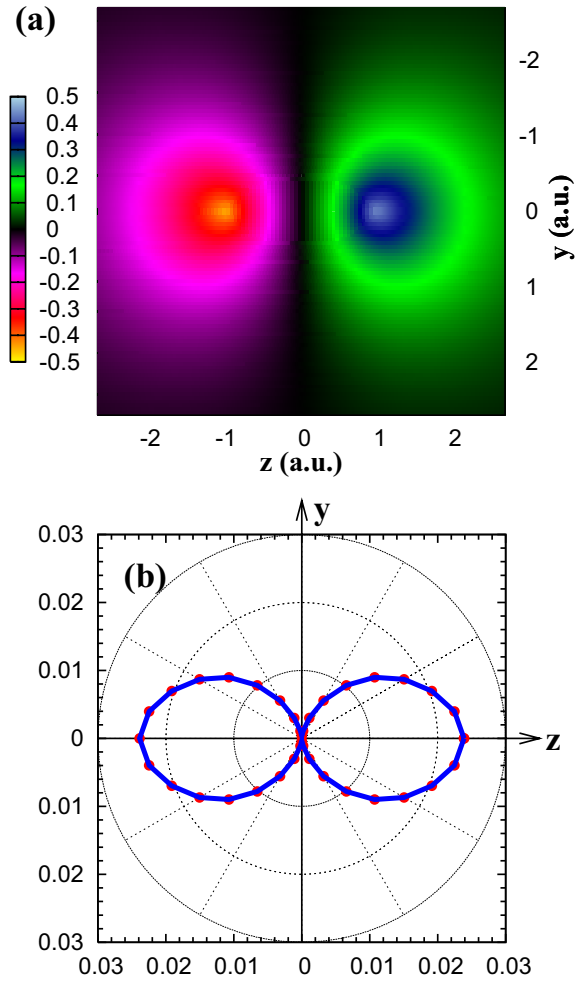

FIG. 2. (Color online) (a) Same as in Fig. 1(a), but for the $1s\sigma_u$ state of H_2^+. (b) Same as in Fig. 1(b) but for H_2^+ initially in the $1s\sigma_u$ state, and for laser parameters $I=10^{14}$ W/cm^2, $\omega=0.057$ a.u., and FWHM$\approx$8 fs.

A_0 is the maximum amplitude, $f(t)$ is the pulse envelope chosen as a cosine-squared throughout this work, ω is the laser frequency, $\mathbf{e}=(\sin\theta)\mathbf{e}_y+(\cos\theta)\mathbf{e}_z$ is the unit vector along the laser polarization axis, $\mathbf{e}_y$ and $\mathbf{e}_z$ are unit vectors along the y and z axes. Therefore, θ is the angle between the molecular axis z and the laser polarization. The TDSE is solved in spheroidal coordinates by expanding the wave function in a complex basis of Laguerre and Legendre polynomials. Details on this approach and on the computation of the ionization probability can be found in Refs. [10,11,17].

We time propagate the TDSE starting from the initial states $1s\sigma_g$, $1s\sigma_u$, $2p\pi_u$, and $2p\pi_g$ of H_2^+. These initial states have different symmetries and electron distributions within their orbital. Contour plots in the (y,z)-plane of electronic wave functions $\Psi(y,z)=\Psi(x=0,y,z)$ are shown for the internuclear distance $R=2$ a.u. in Fig. 1(a) for $1s\sigma_g$, in Fig. 2(a) for $1s\sigma_u$, in Fig. 3(a) for $2p\pi_u$, and in Fig. 4(a) for $2p\pi_g$. At this internuclear distance, the electronic energies of these states are $E_{1s\sigma_g}=-1.1026$ a.u., $E_{1s\sigma_u}=-0.6675$ a.u., $E_{2p\pi_u}=-0.4288$ a.u., and $E_{2p\pi_g}=-0.2267$ a.u.

With the initial state $1s\sigma_g$, whose wave function is plotted in Fig. 1(a), we use a laser of frequency $\omega=0.057$ a.u. ($\lambda=800$ nm), of peak intensity $I=5\times10^{14}$ W/cm^2 and of total pulse duration of about 26 fs. This means that at least 19 photons are necessary to reach the ionization threshold, so that we are in the presence of a multiphoton ionization process. The corresponding ionization probability vs the orientation angle θ is plotted in polar coordinates in Fig. 1(b). It appears that the ionization probability shows a maximum for the parallel orientation ($\theta=0$) of the molecular axis relative to the laser polarization axis, and a minimum for the perpendicular orientation ($\theta=\pi/2$). Considering that enhanced ionization occurs in molecules for parallel orientation due essentially to electron tunnelling between potential wells [6,7], it is not surprising that ionization is maximum for this orientation. In fact, electron tunnelling between potential wells is maximum for the parallel orientation, and gradually decreases with increasing orientation angle θ and disappears for the perpendicular orientation. This explains the maximum ionization obtained for the parallel orientation. Finally, the ionization probability is Fig. 1(b) clearly mimics the contour

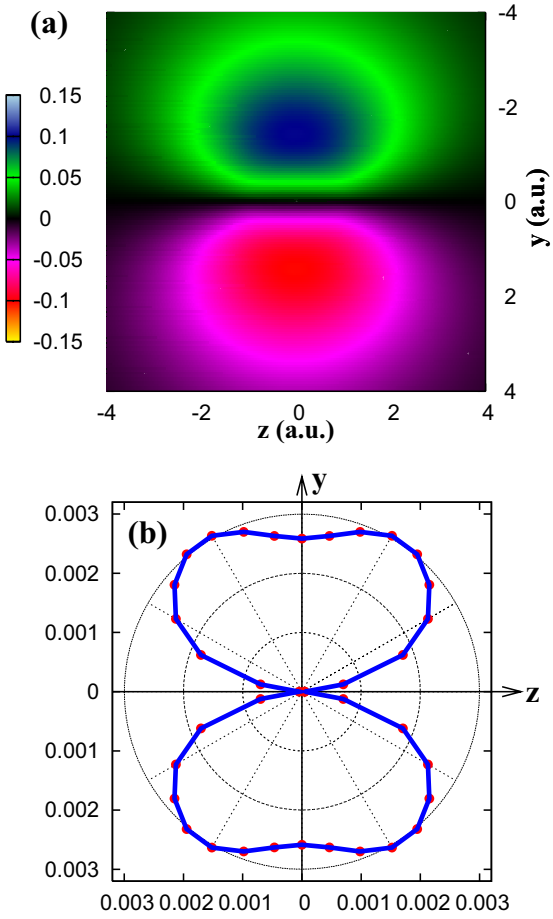

FIG. 3. (Color online) (a) Same as in Fig. 1(a), but for the $2p\pi_u$ state of H_2^+. (b) Same as in Fig. 1(b) but for H_2^+ initially in the $2p\pi_u$ state, and for laser parameters $I=10^{13}$ W/cm^2, $\omega=0.043$ a.u., and FWHM$\approx$11 fs.

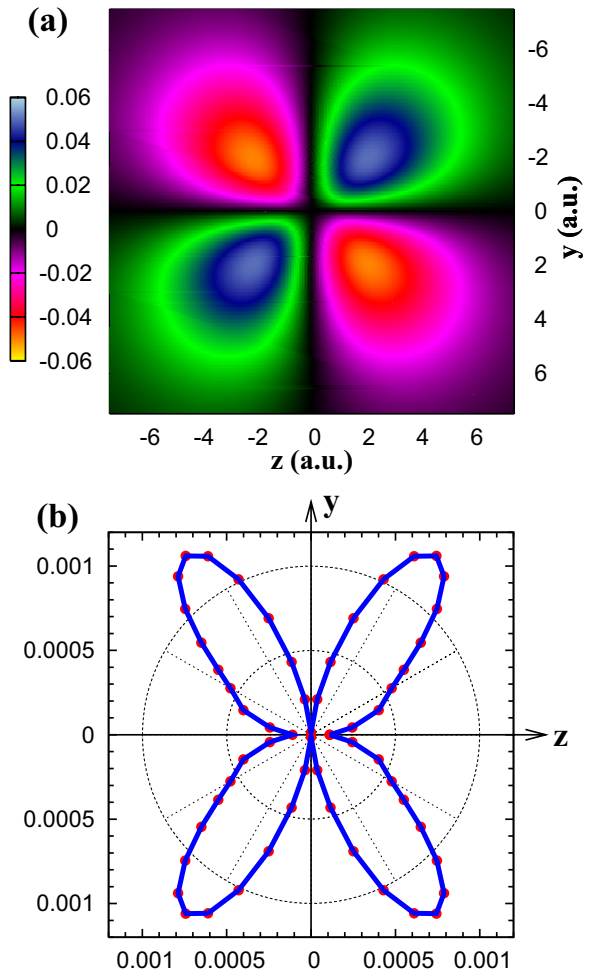

FIG. 4. (Color online) (a) Same as in Fig. 1(a), but for the $2p\pi_g$ state of H_2^+. (b) Same as in Fig. 1(b) but for H_2^+ initially in the $2p\pi_g$ state, and for laser parameters $I=10^{12}$ W/cm^2, $\omega=0.012$ a.u., and FWHM$\approx$19 fs.

of electron distribution in Fig. 1(a). This feature is further illustrated in the next other cases.

Figure 2(b) displays the orientation dependence of the ionization probability obtained with the $1s\sigma_u$ initial state shown in Fig. 2(a). Here, the laser pulse used has a peak intensity $I=10^{14}$ W/cm^2, a frequency $\omega=0.057$ a.u., and a pulse duration of 8 fs at the full width at half-maximum (FWHM) of the pulse envelope. Note that due to symmetry requirements, there is a nodal axis along which the electronic wave function vanishes, with the wave function at the left and at the right of this nodal axis having opposite signs. This nodal axis (i.e., the y axis) is medial to the two nuclei and perpendicular to the internuclear axis. The ionization probability for this case is also maximum for the parallel orientation as for the $1s\sigma_g$ case. However, a strong suppression of ionization occurs for the perpendicular orientation; an orientation in which the laser polarization is parallel to the nodal axis in the $1s\sigma_u$ wave function. The resulting orientation dependence of the ionization shown in Fig. 2(b) also mimics the electron distribution in Fig. 2(a).

The $1s\sigma_g$ and $1s\sigma_u$ electronic orbitals are similar in the sense that the electron cloud is concentrated along the internuclear axis, right around the nuclei. It is expected that the maximum ionization for the parallel orientation is due to interwell tunnelling mechanism mentioned earlier, because electrons in these orbitals are sitting on top of the double-well potential created by the Coulomb attraction of the nuclei. This tunnelling mechanism seems to suggest that both the location of the nuclei and the electron distribution strongly affect the ionization outcome, and that there is no obvious way of disentangling the two contributions. The question now is what happens for electronic states such as the $2p\pi_u$ and $2p\pi_g$ in Figs. 3 and 4, in which the electron cloud is localized off the nuclei due to symmetry restrictions?

The ionization probability obtained with the initial excited state $2p\pi_u$ of H_2^+ is plotted in Fig. 3(b) vs the orientation angle θ. Note that the wave function of the $2p\pi_u$ state has a nodal axis that coincides with the internuclear axis. Since the $2p\pi_u$ state is much closer to neighboring excited states than $1s\sigma_g$ and $1s\sigma_u$, these excited states can be rapidly populated if no precaution is taken, in which case the active orbital becomes a superposition of many orbitals instead, whose image may be difficult to comprehend. To minimize couplings with neighboring excited states, we use a lower laser intensity $I=10^{13}$ W/cm^2 and lower frequency

$\omega=0.043$ ($\lambda=1064$ nm) than in preceding cases. In contrast to the cases of $1s\sigma_g$ and $1s\sigma_u$ active orbitals, the ionization probability in Fig. 3(b) is maximum and nearly flat for $60° \leqslant \theta \leqslant 150°$, but shows a sharp minimum for the parallel orientation of the molecule ($\theta=0$), i.e., when the laser polarization is parallel to the internuclear axis. This indicates that the electron probability distribution in the active molecular orbital has a much stronger influence on the orientation dependence of molecular ionization than the location of the nuclei. In fact, symmetry forces in the $2p\pi_u$ orbital tend to restrict the electron along an axis perpendicular to the internuclear axis, while forcing a nodal structure along the internuclear axis. Interwell tunnelling is significantly suppressed here because electrons are localized off the nuclei. It now appears that the electron distribution concentrated along the internuclear axis plays a greater role in yielding maximum ionization for the parallel orientation for the $1s\sigma_g$ and $1s\sigma_u$ cases than the interwell tunnelling mechanism. Finally, it is also worth noticing that the ionization probability in Fig. 3(b) is an image of the electron distribution contour in the active orbital $2p\pi_u$ in Fig. 3(a).

The electronic wave function for the $2p\pi_g$ orbital in Fig. 4(a) shows interesting features: (i) one nodal axis along the internuclear axis and another along the median axis that intersects perpendicularly with the molecular axis; (ii) the electron cloud is restricted approximately along the diagonals in the (y,z)-plane, resulting in a peak electron distribution along each quadrant of this plane; (iii) the wave function changes sign from one peak distribution to the adjacent one. In order to minimize resonances with neighboring excited states, we further decrease the laser intensity and frequency to $I=10^{12}$ W/cm^2 and $\omega=0.02$ a.u. One sees in Fig. 4(b) that the ionization probability is seriously cancelled for molecular orientations parallel to nodal axes. Ionization appears to be maximum for orientation angles $\theta \approx 50°$ and $\theta \approx 140°$, orientation angles at which the laser polarization overlaps with major axes of electron distribution. Therefore, as for the case of the $2p\pi_u$ initial state, the influence of electron distribution on the orientation dependent ionization probability dwarfs that of the nuclei location. Here again, the resulting ionization probability reproduces the contour of the electron distribution.

Results in Figs. 1–4 indicate that the ionization probability as a function of the orientation angle provides an approximate image of the contour of the electron distribution within the active molecular orbital. This feature appears to be sustained despite the variety of active orbitals and laser parameters considered in this work. However, we expect that for laser intensities and frequencies such that there is a strong resonant coupling of the initial state with neighboring states, the active orbital becomes a superposition of eigenstates, which leads to an ionization probability that may not mimic the electron distribution in the initial state. The fact that the orientation dependence of ionization mimics the electron distribution arises from two features: The first is that ionization tends to maximize when the laser polarization is parallel to a molecular axis along which the electron cloud is maximally localized; the stronger the electron distribution along the laser polarization, the larger the ionization rate. The second feature is that the ionization is significantly suppressed when the linear polarization of the laser is parallel to a nodal axis along which the electron distribution vanishes.

All results discussed above for the $1s\sigma_u$, $2p\sigma_u$, and $2p\sigma_g$ illustrate a strong suppression of ionization for molecular orientations for which the laser field is parallel to the nodal axis in the active orbital. Note that the wave function is antisymmetric with respect to all nodal axes, and when the laser pulse is linearly polarized along this axis, the wave function preserves this antisymmetric character, which leads to destructive interferences as illustrated in Ref. [15]. As the angle between the nodal axis and the laser polarization increase, the antisymmetry of the system with respect to the nodal axis is broken, leading to an increase of ionization due to a decrease in the ionization suppression. Finally, it is worth mentioning that all polar plots of the ionization probability in this paper are in absolute scale.

III. MAPPING ELECTRON DISTRIBUTION WITH IONIZATION FOR THE $2P\pi_G$ STATE

We have seen in the preceding section that the ionization probability tends to maximize when the laser polarization is parallel with a particular axis of the molecule along which the electron is concentrated. This is the case along the internuclear axis z for the $1s\sigma_g$ and $1s\sigma_u$ states in Figs. 1 and 2, along the axis perpendicular to the internuclear axis for the $2p\pi_u$ state in Fig. 3, and approximately along the two diagonals in Fig. 4 for the $2p\pi_g$ state. Note that for the $2p\pi_g$ orbital, electrons are also concentrated in the directions parallel and perpendicular to the internuclear axis, but ionization is suppressed for laser pulses linearly polarized along these directions due to destructive interferences.

For molecular orientations where the ionization probability tends to maximize, the electronic wave function is symmetric with respect to the major axis of electron distribution (see, e.g., the z axis in Figs. 1 and 2, the y axis in Fig. 3, and the diagonals in Fig. 4). When the laser polarization is parallel with these major axes of electron distribution, the system preserves its spatial symmetry, in which case there is no ionization suppression and the ionization is maximal and atomiclike. Therefore, we may conclude that the ionization probability maximizes when the laser polarization axis overlaps with a major axis of electron distribution in the active orbital, provided that the orbital is spatially symmetric with respect to this axis. In order to illustrate this, we consider the

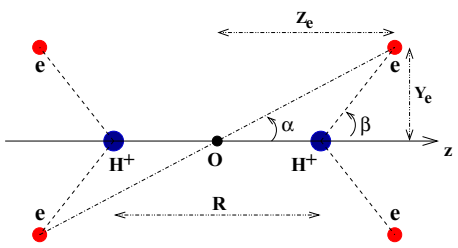

FIG. 5. (Color online) Schematic representation of the $2p\pi_g$ orbital of the H_2^+ molecule, where the two large (blue) dots represent the nuclei and the four small (red) dots represent the four peaks in the electron distribution.

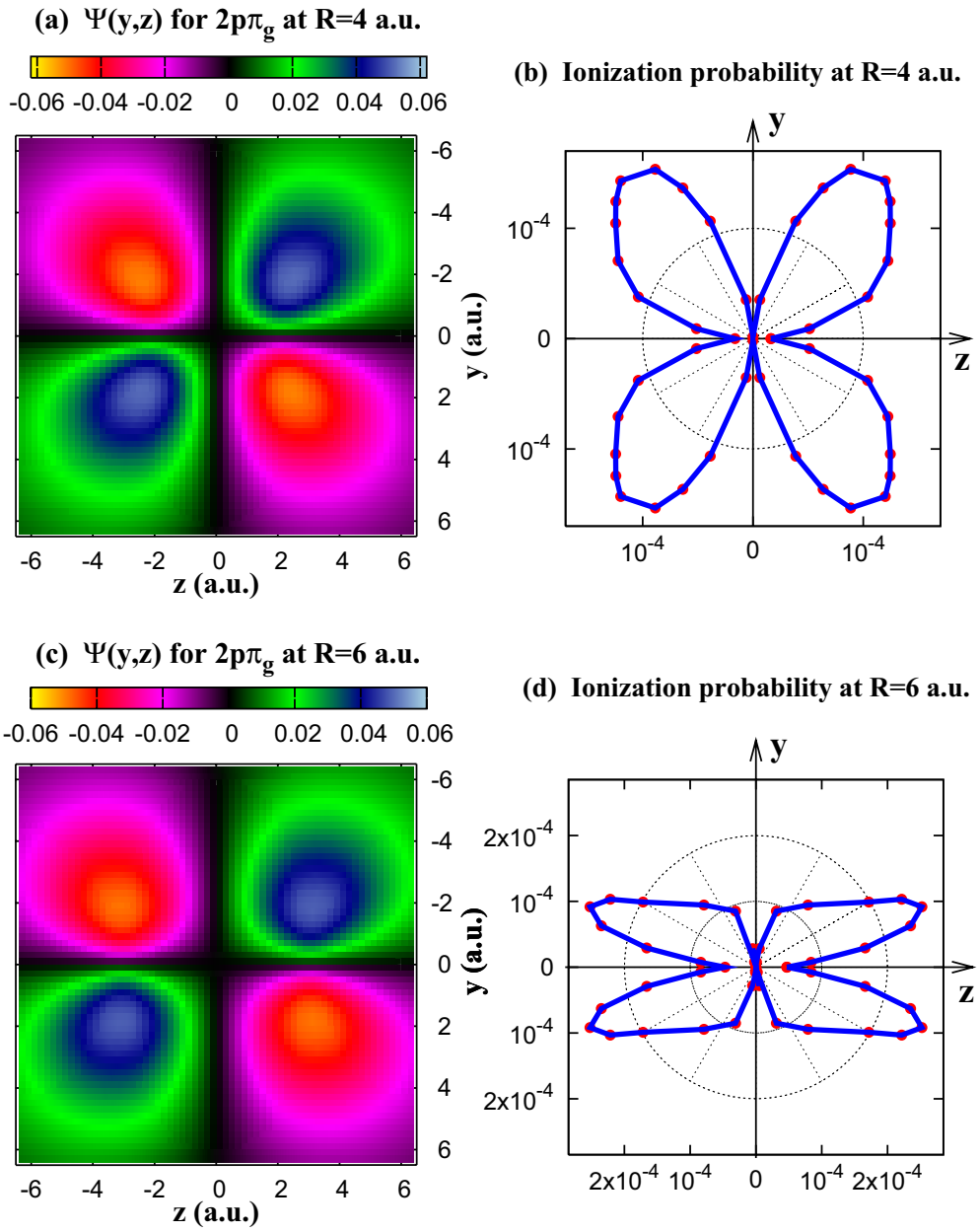

FIG. 6. (Color online) Left plots show contour plots of the wave function $\Psi(y,z)$ of the $2p\pi_g$ state of H_2^+ at two internuclear distances R: (a) for $R=4$ a.u.; (c) for $R=6$ a.u. Right plots display the orientation dependence of the ionization probability obtained with the active orbital shown on the corresponding left plot. Laser parameters are the same as in Fig. 4.

case in which the $2p\pi_g$ is the initial state, but with increasing internuclear distance. With increasing internuclear distance, the electron cloud in the $2p\pi_g$ is distorted, and if our assertion above is true, the resulting orientation dependence of ionization probability should reflect this distortion.

A schematic representation of the $2p\pi_g$ orbital of the H_2^+ molecule is shown in Fig. 5. We have computed the $2p\pi_g$ wave function of H_2^+ for various internuclear distances R, and in each case we have extracted the coordinates Y_e and Z_e at which peaks of electron distribution occur in the wave function. Results are summarized in Table I for Y_e, Z_e, as well as for the angles $\alpha=\arctan(Y_e/Z_e)$ and $\beta=\arctan\{Y_e/[(Z_e-R)/2]\}$. The major axis of electron distribution along which the wave function is symmetric is the line that connects two diagonal peaks. This axis make the angle α with the molecular axis. One sees that with increasing R, the z coordinate of the peak of electron distribution Z_e increases rapidly, while its y coordinate Y_e changes rather slowly. It follows that with increasing R, electrons are increasingly localized along the molecular axis, in other words the angle α decreases with R [Figs. 6(a) and 6(c) also illustrate this feature].

The orientation dependence of the ionization probability obtained with the $2p\pi_g$ as the active orbital is illustrated in Fig. 6 for the $R=4$ a.u. and $R=6$ a.u. It is remarkable that the minima in ionization for the parallel and perpendicular orientation of the molecule occurs independently of the internuclear distance, which indicates that ionization suppression at

TABLE I. Coordinates X_e and Y_e (illustrated in Fig. 5) giving the location of peaks in the electron distribution in the $2p\pi_g$ orbital for various internuclear distances. The corresponding angles α and β are also given.

R (a.u.)	Y_e (a.u.)	Z_e (a.u.)	α (deg)	β (deg)
0.3	2.12	2.12	45.00	47.10
0.5	2.11	2.12	44.86	48.45
1.0	2.07	2.11	44.45	52.13
2.0	1.97	2.12	42.90	60.38
3.0	1.87	2.22	40.11	68.94
4.0	1.83	2.44	36.87	76.48
5.0	1.83	2.75	33.64	82.22
6.0	1.85	3.12	30.67	86.29

these angles is independent of the electronic structure and depends only on the orbital symmetry. In contrast, the maxima in ionization depend strongly on R. One sees that with increasing R, these maxima occur at smaller angles, about 50° for $R=2$ a.u. in Fig. 4, about 45° for $R=4$ a.u. in Fig. 6(b), and about 25° for $R=6$ in Fig. 6(c). These angles correspond to molecular orientation angles close to the corresponding angles α in Table I. This indicates that maximum ionization occur indeed at molecular orientations for which there is a maximum overlap between laser polarization and electrons in the active orbital. This shows that the orientation dependence of the ionization probability approximately maps the electron distribution in the molecular orbital.

IV. CONCLUSIONS

We have investigated the influence of orbital symmetry and electron distribution on the orientation dependence of molecular ionization, using an *ab initio* solution of the corresponding time-dependent Schrödinger equation (TDSE). Our choice for H_2^+ is motivated by the fact that it is the only molecule for which an exact numerical solution for the TDSE is possible with current computer resources. We have propagated the TDSE, starting from initial states (active orbitals) $1s\sigma_g$, $1s\sigma_u$, $2p\pi_u$, and $2p\pi_g$ of H_2^+, which have various symmetries and electron density distributions. It is found that when the molecule is oriented such that laser polarization is parallel to a nodal axis of the active orbital, the ionization probability is strongly suppressed due to destructive molecular interferences [15]. The occurrence of such destructive interference is due to the fact that the system is spatially antisymmetric relative to the nodal axis. On the other hand, the ionization probability tends to maximize when the molecule is oriented such that the laser polarization is parallel to a molecular axis along which the electron distribution is concentrated, provided that the active orbital is spatially symmetric with respect to this axis.

For the most interesting $2p\sigma_g$ state, we show that the ionization suppression is sustained at various internuclear distance R, which indicates that this effect is essentially a symmetry related effect. Also, with increasing R, the electron density distribution becomes increasingly located along the internuclear axis, in other words, as R increases the major axes of electron distribution make an increasingly small angle relative to the internuclear axis. Our results show that as R increases, the maximum in the orientation dependence of the ionization probability occurs at increasingly small angles relative to the internuclear axis. This clearly shows that the orientation dependence of the ionization probability maps the electron distribution in the active orbital, thereby allowing to image the contour of electron density distributions in molecules.

ACKNOWLEDGMENTS

The authors thank the Natural Sciences and Engineering Research Council of Canada (NSERC) and the Canadian Institute for Photonics Innovation (CIPI) for their financial support.

[1] A. D. Bandrauk and S. Chelkowski, Phys. Rev. Lett. **87**, 273004 (2001).
[2] G. Binnig, H. Rohrer, C. Gerber and E. Weibel, Phys. Rev. Lett. **49**, 57 (1982).
[3] C. E. Brion, G. Cooper, Y. Zheng, I. V. Litvinyuk, and I. E. McCarthy, Chem. Phys. **270**, 13 (2001).
[4] J. Itatani, J. Levesque, D. Zeidler, H. Niikura, H. Ppin, J. C. Kieffer, P. B. Corkum, and D. M. Villeneuve, Nature (London) **432**, 867 (2004).
[5] P. B. Corkum, Phys. Rev. Lett. **71**, 1994 (1993).
[6] T. Zuo and A. D. Bandrauk, Phys. Rev. A **52**, R2511 (1995).
[7] T. Seideman, M. Y. Ivanov, and P. B. Corkum, Phys. Rev. Lett. **75**, 2819 (1995).
[8] G. L. Kamta and A. D. Bandrauk, Phys. Rev. Lett. **94**, 203003 (2005).
[9] I. V. Litvinyuk, K. F. Lee, P. W. Dooley, D. M. Rayner, D. M. Villeneuve, and P. B. Corkum, Phys. Rev. Lett. **90**, 233003 (2003).
[10] G. L. Kamta and A. D. Bandrauk, Phys. Rev. A **70**, 011404(R) (2004).
[11] G. L. Kamta and A. D. Bandrauk, Phys. Rev. A **71**, 053407 (2005).
[12] C. D. Lin, X. M. Tong, and Z. X. Zhao, J. Mod. Opt. **53**, 21 (2005).
[13] A. Talebpour, C. Y. Chien, and S. L. Chin, J. Phys. B **29**, L677 (1996).
[14] C. Guo, M. Li, J. P. Nibarger, and G. N. Gibson, Phys. Rev. A **58**, R4271 (1998).
[15] J. Muth-Böhm, A. Becker, and F. H. M. Faisal, Phys. Rev. Lett. **85**, 2280 (2000).
[16] H. Stapelfeldt and T. Seideman, Rev. Mod. Phys. **75**, 543 (2003).
[17] G. L. Kamta and A. D. Bandrauk, Laser Phys. **15**, 502 (2005).